

TRACK STRUCTURES IN AN URBAN ENVIRONMENT

Prof.dr.ir. C. Esveld

Professor of Railway Engineering, TU Delft

Symposium K.U. Leuven

September 1997

TABLE OF CONTENTS

| | | |
|------------|---|-----------|
| 1. | INTRODUCTION | 1 |
| 2. | TRACK STRUCTURES | 2 |
| 2.1 | Tram tracks | 2 |
| 2.1.1 | Concrete slab as the foundation for tram tracks | 2 |
| 2.1.2 | Pavement | 3 |
| 2.1.3 | Nikex | 3 |
| 2.1.4 | Embedded rail | 4 |
| 2.1.5 | Open tram track systems | 4 |
| 2.1.6 | Grass track | 4 |
| 2.2 | Track on structures | 5 |
| 2.2.1 | Construction principles | 5 |
| 2.2.2 | Types of structures | 5 |
| 2.3 | track resilience | 7 |
| 3. | DYNAMIC PRINCIPLES | 8 |
| 3.1 | General | 8 |
| 3.2 | One mass spring system | 8 |
| 3.3 | Wheel/rail forces | 10 |
| 3.4 | Track modelling. | 11 |
| 3.4.1 | General considerations | 11 |
| 3.4.2 | Transfer function between track load and track displacement. | 11 |
| 3.4.3 | Beam on an elastic foundation | 12 |
| 3.4.4 | Double beam. | 14 |
| 3.4.5 | Discrete support | 15 |
| 3.5 | Vertical wheel response | 15 |
| 3.5.1 | Hertzian contact spring. | 15 |
| 3.5.2 | Transfer functions between wheel and rail. | 15 |
| 3.5.3 | Analysis of paved-in tram track structure | 18 |
| 3.6 | Embedded rail construction | 19 |
| 4. | REFERENCES | 21 |

1. INTRODUCTION

In this paper track structures in an urban environment will be discussed. In addition to tracks in the open paved-in structures are treated for tram and light rail. Also attention is paid to solutions in tunnels. The information is primarily based on a study carried out by TU Delft for CROW entitled Concrete in Railway Structures [1] and on lectures and publications of TU Delft [2,3]

In the second part some aspects of track dynamics are addressed based on graduate courses given at TU Delft [4,5]. When dealing with track mechanics in fact most of the problems are related in one way or another to dynamics. The 1-mass spring system can be regarded as the most elementary system, with the aid of which a number of practical problems can be considered. Extensions can be made in two directions: the construction can be enhanced to a multi degree of freedom system, and the load can be made more complex in terms of impact loads, and loads with a random character.

Track and rolling stock should in fact not be considered separately, but as one consistent system. For this reason the interaction between vehicle and track is introduced here, without going into all the details required for a full treatment of this complex matter. After an introduction of the Hertzian spring the transfer function between wheel and rail is derived.

An application with the discrete element model TILLY, developed at the Mechanics Section of TU Delft, to study the dynamic behaviour of paved-in track is discussed. Besides, some measurement results of the dynamic behaviour of an Embedded Rail Construction are presented.

2. TRACK STRUCTURES

2.1 Tram tracks

On open tram tracks wooden sleepers, embedded in porphyry ballast) are giving way to twin-block concrete sleepers which, being heavier, enhance track stability.

Most types of paved-in track (i.e. those over which road vehicles *can* run) include a continuous concrete foundation slab under their entire length. Directly or indirectly, this slab is responsible for transmitting the vertical and horizontal forces emanating from tram and road traffic. Track re-alignment is almost or completely unnecessary, depending on the system used to secure the rails. A continuous slab also has the advantage that it spreads the load, bridging sections of the subgrade less able to bear load. No form of discontinuous support could be used for paved-in tram track structures, because road traffic requires a continuous surface to run on. What *would* be possible is a system incorporating sleepers covered over by concrete slabs, which would then provide the pavement. The disadvantage of this would however be that maintenance work on the sleepers (i.e. re-alignment) would require removal of the slabs. Often, therefore, the continuous concrete slab is the only possible option for paved-in tram tracks.

2.1.1 Concrete slab as the foundation for tram tracks

During construction of new lines, the first step is to dig a trench; the quality of the ground may also be improved at this stage. The concrete is then poured in situ, forming an un-reinforced slab. The concrete quality varies between B17.5 and B22.5 and the slab is approx. 0.3 m thick. Once the concrete has hardened, the rails can be laid. Various options are possible. In Amsterdam, Hakorit (plastic) plates bring the Ri60 grooved rails to the right height, following which threaded studs and steel plates secure them to the base. The only elastic element in this system is a triple spring washer.

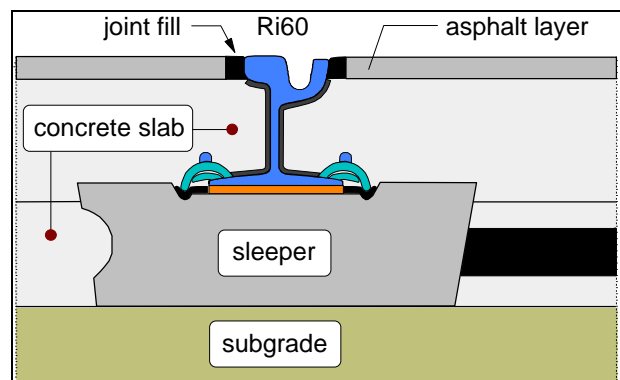


Fig. 1. Concrete sleepers used on tram track to speed up construction work

To speed up the construction process, another technique utilizes concrete twin-block sleepers, to which the rails are secured using Vossloh spring clips (Fig. 1.). A cork-rubber pad is inserted between the rail and the concrete sleeper to filter out dynamic high-frequency oscillations, an essential precaution to protect the concrete sleeper. After the track has been aligned, the concrete sleepers are embedded into a continuous concrete slab, giving the same effect as the first method. The second method is more expensive, on account of the comparatively expensive sleepers, but has the advantage of a considerable reduction in construction time. This means less disruption to the tram service, especially when existing track is being renewed.

In The Hague, a special plastic pad has been developed, and is inserted between the rail and the concrete slab (Fig. 2.). Before the concrete is poured, the track panels are supported temporarily on small concrete plates and blocks. The plastic pads to be embedded in the concrete, on which the studs are mounted, are already clamped to the underside of the rail, in the gaps between the temporary supports (the studs consist of heavy-duty M22 bolts, placed head-down and embedded in the slab).

Wooden wedges adjust the rails to approximately the right height. Like vertical alignment, lateral alignment must be correct to within certain toler-

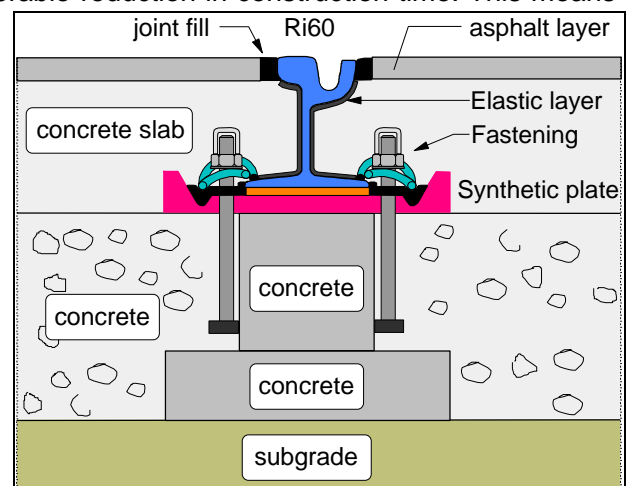


Fig. 2. Hague design. The rails are laid on plastic pads.

ances. The plastic pads make it possible to adjust both top and alignment later. Once the concrete has been poured and has had time to harden, the track is adjusted to its final vertical position (using shims) and horizontal position (using plastic wedge devices), after which the Vossloh spring clips are secured to the studs.

2.1.2 Pavement

So far, there has been no mention of the pavement. Many options are possible, almost all of which are independent of the concrete slab. In The Hague and in Rotterdam, both asphalt and cobbles are in general use. In Amsterdam, prefabricated concrete slabs have been in use for over ten years – the “Vinnese System”.

If the pavement is to consist of asphalt, most of the space on top of the continuous concrete slab on which the rails are laid is filled with un-reinforced concrete. An elastic material is inserted between the rail and the concrete, to allow the rail a certain degree of free movement. Any fastenings are covered over with plastic caps before the concrete is poured. A depth of 4 cm is allowed on top of the concrete for the asphalt. Like the concrete, the asphalt is not poured right up to the rail – a narrow gap is left, which will be filled later with a bitumen compound.

Cobbles are generally used where “they” (usually the authorities) consider that aesthetics require them. From a technical point of view, cobbles have nothing to offer but disadvantages compared with asphalt. Laying and maintaining them is more expensive, and maintenance is required more frequently. A cobbled surface on a dual-purpose tram/bus route will require particularly regular and expensive maintenance. In addition to all of which, road traffic generates more noise on cobbles than on asphalt. The prefabricated concrete slab pavement used in Amsterdam was chosen primarily on account of the restricted space in the city. It is virtually impossible to divert road traffic, which means that track replacement must be carried out in as short a period as possible. The prefabricated slabs can be removed and replaced rapidly – more rapidly than in the case of the other systems cited earlier. Furthermore, some 90% of the slabs can be re-used after track replacement.

2.1.3 Nikex

On any tram system, the time will eventually come when part of the network has aged to the point that it requires replacement. This may involve replacing the entire structure, or only parts of it, such as the rails and/or pavement. In all cases, the work will cause inconvenience to tram passengers, road users and residents. One solution to this is the Nikex system, developed a few years ago in Hungary (Fig. 3.). Two test lines were built in the Netherlands in the early 1980s.

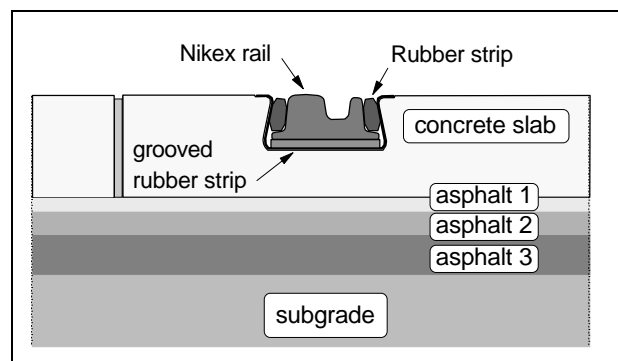


Fig. 3. The Nikex system.

The Nikex system consists of a slab of high-quality concrete. The slab is relatively thin (18 cm) and is therefore reinforced. It has a maximum length of 6 m and is designed to take a single track. Two steel-lined swallowtail channels are let into the slab. The special 7 cm high block rails are laid in these channels on a corrugated rubber mat and then secured with rubber strips pressed into the gaps on either side of the rail. The slabs are laid on a suitable foundation, usually consisting of a number of layers of asphalt, although other types of foundation are possible. As the slabs are not joined together, one of the requirements for the foundation is that it prevent the development of unacceptable differences in height between them.

The transition to existing (stiffer) track is still a problem. No practical solution has yet been produced to the problem of absorbing this difference in stiffness. In The Hague, problems also arose due to vibrations being transmitted from the tram track to nearby flats. Investigation revealed that the natural frequencies of the tram wheels, the track and the foundations of the flats were very close to each other, causing resonance effects. Since that time, the rails have been replaced, both in The Hague and in Rotterdam. In both cases, the operation went very smoothly, with several hundred meters of rail being replaced in a single night. The absence of drilling meant the work could be carried out without creating noise and without disrupting tram and road traffic. Replacing rails laid in the normal fashion, in an as-

phalt pavement, would have taken a good three to five weeks from start to finish, with all the noise and disruption to traffic that would have involved.

2.1.4 Embedded rail

Another method that allows easy replacement of the rails and can also reduce vibration and noise to a significant degree is the embedded rail (Fig. 4.). In this system, the rail is moulded into a channel, using an elastic compound. The channel may be made of steel or concrete – this has no effect on its functioning. The elastic compound generally consists of a polymer, to which cork granules are added. The compound is not affected by oil or chemicals.

The advantage of the embedded rail system is that the rail can move elastically, while the rigid channel ensures these movements have no effect on the structure outside it. This eliminates one major disadvantage of the systems discussed earlier in this chapter that included asphalt pavements (for instance); the joint between the rail and the pavement, generally filled with bitumen, which deteriorates rapidly under the effects of rail movement.

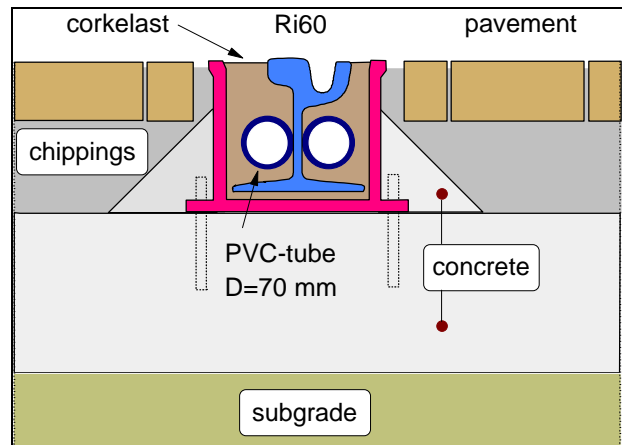


Fig. 4. Embedded rail for a tram system.

The rail must be laid with a high degree of precision, as no further corrections will be possible once it has been moulded into place. The rail is placed in the channel before the compound is poured in; hardened blocks of the same compound are used to hold it in position temporarily. The rails are brushed down and then painted with a primer designed to improve the bond between rail and compound. The channel is then filled with the compound and after a few hours hardening the track is ready to take full operational loads.

2.1.5 Open tram track systems

Tram tracks which, by virtue of their design, are not suitable for road traffic, are known as open tram track systems. Track laid on sleepers embedded in porphyry ballast is an example of an open tram track system. The sleepers may be steel, wood or concrete, although steel is little used nowadays, except in special applications (see “Grass track” below).

In recent years, concrete sleepers have steadily been replacing the traditional wooden sleeper. In the case of tram tracks, the twin-block type is used, consisting of two concrete blocks – to which the rails are fastened – joined together by a steel tube. The advantage of the concrete sleeper lies in its greater mass and superior resistance to lateral shear forces, enabling it to sit securely in the ballast.

The trend over the last few years has been to produce increasingly heavy sleepers.

One disadvantage of concrete sleepers as against wood is that if a single sleeper has to be replaced – which is usually done manually – maintenance personnel have to move a much heavier object by hand.

2.1.6 Grass track

A sleeper-and-ballast tram track does not always make a positive contribution to urban aesthetics, and this has prompted tram operators to consider alternatives in certain areas. The grass track is an attractive substitute for ballasted track; the track looks more natural, and is hence perceived as being more environment-friendly. Its disadvantage is that construction and maintenance can be considerably more expensive than for conventional ballasted track. Various versions are in use. In The Hague, a method has been developed that is very suitable for streets where trees grow close to the track. The “pile design” consists of concrete piles, into which a steel profile is embedded. The foot of the pile is rectangular, with the long sides parallel to the track.

Steel sleepers are fastened between the piles. Their height can be adjusted using a wedge device and their horizontal alignment by means of adjusting bolts. This means that top and alignment can be re-adjusted later (e.g. during maintenance).

The plastic pad used elsewhere in The Hague (on paved-in track laid on a continuous concrete slab) is also used here. The plastic pad is laid on the steel sleeper, with a cork rubber pad on top, followed by

the grooved rails. These are secured by a Vossloh clip. Here again, the plastic pad allows a certain degree of freedom to adjust the lateral alignment of the rails. The space between the piles is filled with sand, with a layer of soil on top. This extends to approx. 5 cm below the top of the rail. Grass seed is sown into the soil, after which the grass itself requires no further maintenance – the passing trams “mow” it.

One feature of this design is the large number of components required to provide adjustability, making the system more expensive. Maintenance of this type of grass track is also expensive. Maintenance personnel have to dig down a number of centimeters to reach the wedge device located between the pile and the sleeper. In practice, the bolts used to adjust lateral alignment rust solid and/or shear off when one attempts to undo them. This also applies to the bolts that hold the vertical adjustment wedges in position.

An alternative is to use a continuous concrete slab, with a layer of soil on top, in which the grass seed can be sown. To allow adequate drainage, however, holes must be made in the slab. This design has been used in both The Hague and Amsterdam, but drainage has proved to be a problem. It may be possible to increase the diameter of the holes, or their number per running meter. Too little is known about the effect of tree roots on this “perforated slab” as yet.

2.2 Track on structures

2.2.1 Construction principles

There are two approaches to laying track on engineering structures. The first is to use a continuous ballast bed (sleepers/porphyry ballast). The second is to lay the track directly on the structure. In this second case, the rails are simply secured to the concrete deck using just a few components. However, sufficient resilience should be a point of great concern. The advantage of fixing the rails directly to the structure is that it reduces height, both because the thick ballast bed is replaced by relatively thin fastenings, and because the reduced mass of the track structure overall allows the dimensions of the supporting structure (the bridge) to be reduced.

2.2.2 Types of structures

Many different types of ballastless track are currently in use around the world. For railways light rail and trams these structures do not differ fundamentally.

Ballastless track is undergoing rapid development in Germany. Since 1996, DB has been operating a test track in Karlsruhe consisting of seven new types of ballastless track [6,7,8,9]. The best-known German designs are the Rheda and the Züblin [10], named after the places where these types were first used. In both of these systems, the sleepers are cast into a concrete slab.

The Stedef system, illustrated in Fig. 5, is most often used in tunnels and metro systems and is the most common application. A rubber boot under the sleeper provides a high degree of elasticity, which ensures good noise and vibration insulation [11].

The Sonnevile Low Vibration track is closely related to the Stedef system. This

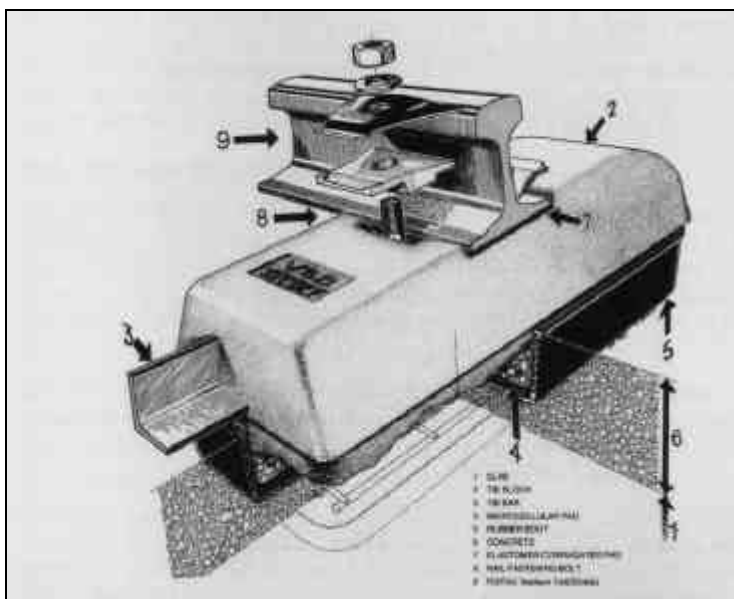


Fig. 5 Stedef Twinblock system

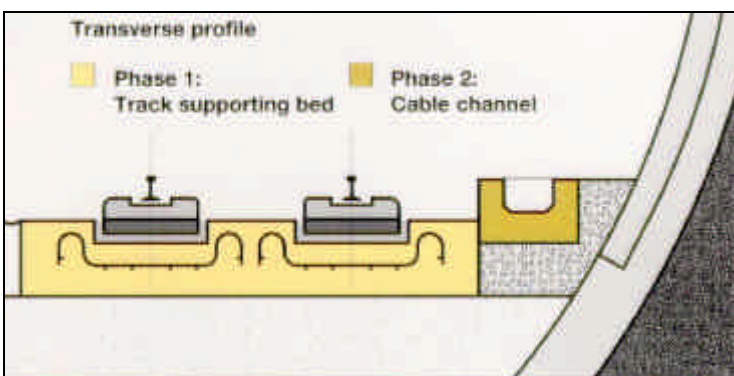


Fig. 6 Swiss system

is a block track design, which, like Stedef, also uses a rubber boot. Applications include the Channel Tunnel.

Another twinblock variant related to Stedef is the Swiss system depicted in Fig. 6, mainly used in tunnels. A special slipform paver lays a concrete slab, following which the sleepers – fitted with rubber boots – are placed in position and cast into place [12].

The Edilon block track system (Fig. 7) falls into the same category, and is mainly used for bridges and tunnels. Under this (top-down) system, the first step is to place the rails and blocks in position. The blocks are then cast in using Corkelast, to provide the necessary elastic support. Important applications include 100 km on NS and light rail systems in the Netherlands and the Madrid metro (approx. 100 km).

In Japan, ballastless track always consists of prefabricated slab track, using slabs just under 5 m long. The percentage of ballastless track varies considerably from line to line. The newer lines include a higher percentage (up to 96%). The slab track design has remained virtually unchanged since the first sections were laid in 1972 [13].

ÖBB (Austria) has 25 km of ballastless track, mainly in tunnels and on viaducts. The ÖBB-Porr system, comprising embedded monoblock sleepers enclosed in rubber, is very similar to the Züblin design mentioned above. There is also a variant using prefabricated slabs (the Porr system).

All the designs mentioned so far were based on the rail being supported at discrete points – the sleeper principle. Since 1976, a continuously supported rail system has been in use in the Netherlands on a small scale. The system is known as the Embedded Rail Construction (ERC), and involves providing continuous support for the rail by means of a compound consisting of Corkelast (a cork/rubber mixture) (Fig. 8.). The great advantage of this design is that the track is built “top-down”, which means that tolerances in the supporting structure have no effect on the track geometry obtained. NS now has 20 years experience with this system, and it has proved to require little maintenance. As said previously, also the Public Transport operators in The Netherlands have positive experience with this structure.



Fig. 7 Detail of Edilon Block System with Pandrol fasteners

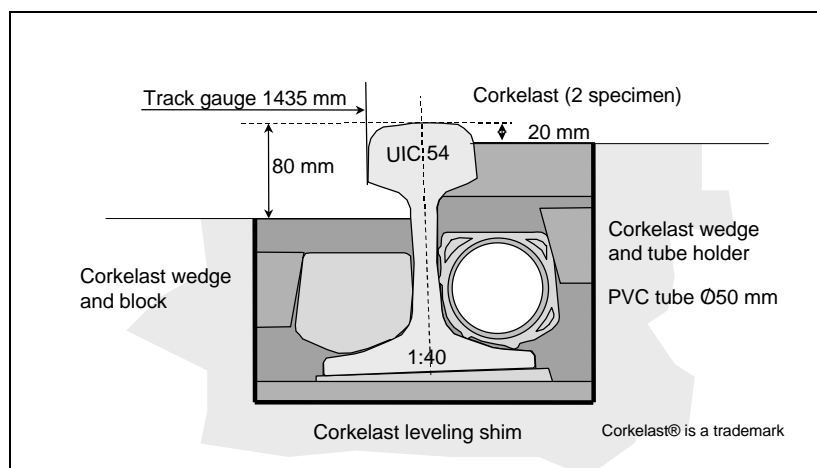


Fig. 8 Details of embedded rail structure

2.3 track resilience

On ballasted track, approximately half the resilience needed to absorb dynamic forces is provided by the ballast bed and the other half by the sub-grade. Ideally, the stiffness of the overall track structure should be at least of the order of 100 kN/mm, which equates to the structure deflecting 1 mm under a 20 t axle load.

High frequency vibration is filtered out by a rail pad inserted between the rail and the sleeper. This cork rubber or rubber component allows the use of relatively stiff concrete sleepers, which are susceptible to scratching.



Fig. 9. Elastic rail support in track structure, Berlin

On slab track, and on bridges where the rails are fixed down directly, additional resilience must be added to the system to compensate for the absence of ballast. In principle there are two ways of achieving this:

- Adding extra resilience under the rail by, for instance, inserting extra thick rail pads (Fig. 9) or by using ERC
- Inserting a second resilient layer under the supporting blocks or the sleepers.

In the second case, a two-mass spring system is effectively created, with a primary and secondary spring, analogous to a vehicle. Fig. 10 shows the principle. TU Delft is currently studying the difference in the dynamic behaviour of these types of track.

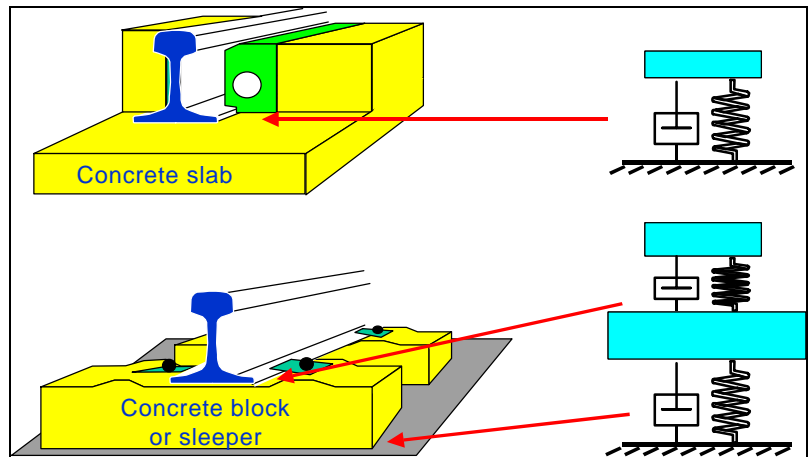


Fig. 10 Principle of spring system in track

3. DYNAMIC PRINCIPLES

3.1 General

When considering dynamic aspects of track one should realize that dynamics is in fact the interaction between load and structure. Loads vary in time and the way this happens determines the character of the load. Generally speaking distinction can be made between periodic loads, impact loads and stochastic loads.

Structures are characterized by their frequency response function, governed by mass, damping and stiffness [14]. These parameters determine the natural frequencies of the structure, in other words those frequencies in which the structure likes to vibrate. If the loads contain frequency components corresponding to the natural frequencies of the structure, large dynamic amplifications may occur. The general term used for this is resonance.

Dynamic behaviour is governed by the law of momentum, which says that force equals the change of momentum, or:

$$K = \frac{d(mv)}{dt} \quad (2.1)$$

When the mass is constant this equation transforms into Newton's law saying force equals mass times acceleration:

$$K = ma \quad (2.2)$$

3.2 One mass spring system

The most simple construction is the so-called one mass spring system presented in Fig. 11. This single degree of freedom system is governed by the following equation:

$$m\ddot{x} + c\dot{x} + kx = F(t) \quad (2.3)$$

For the response to a harmonic force the solution is of the form:

$$x(Wt) = H(W)F(Wt) \quad (2.4)$$

The so-called transfer function H reads:

$$H(W) = \frac{\frac{1}{k}}{\sqrt{\left(1 - \frac{W^2}{w^2}\right)^2 + \left(2V\frac{W}{w}\right)^2}} \quad (2.5)$$

in which:

$$V = \frac{c}{c_{cr}} \quad (2.6)$$

$$\begin{aligned} c_{cr} &= 2\sqrt{km} \\ &= 2mw \end{aligned} \quad (2.7)$$

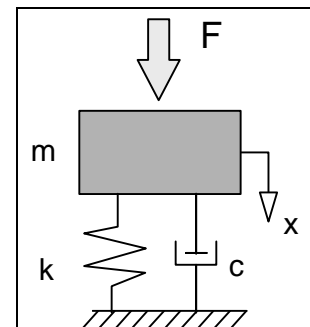


Fig. 11. 1 mass spring system

The transfer function describes the relationship between response and excitation in the frequency domain. When the force as function of time is known a Fourier transform can be made and the response then simply follows from a multiplication of the transformed force by the transfer function. An other way of achieving this result is by using the convolution integral, also known as Duhamel integral, which is represented by:

$$x(t) = \int_0^t F(t)h(t-t)dt \quad (2.8)$$

In this equation h is the unit impulse response function, which is the response to a unit impulse load. The unit impulse response function depends on the construction properties and reads:

$$h(t-t) = \frac{e^{w(t-t)}}{mw\sqrt{1-V^2}} \sin(\sqrt{1-V^2} w(t-t)) \quad (2.9)$$

From this expression it is obvious that the response calculation in the time domain is quite complicated compared to the calculations in the frequency domain. In the frequency domain it was found that:

$$X(f) = H(f)F(f) \quad (2.10)$$

The unit impulse response function h and the transfer function H are related via a Fourier transform:

$$h = FT(H) \quad (2.11)$$

$$H = FT^{-1}(h) \quad (2.12)$$

in which FT stands for Fourier transform and FT^{-1} for inverse Fourier transform.

With vehicle track interaction excitations are induced by irregularities in the wheel rail interface. In the most simplified form this can be considered as forced displacements, the principle of which is illustrated in Fig. 12. The equation of motion reads:

$$m\ddot{x} + c\dot{x} + kx = c\dot{y} + ky \quad (2.13)$$

or alternatively:

$$m\ddot{z} + c\dot{z} + kz = -m\ddot{y} \quad (2.14)$$

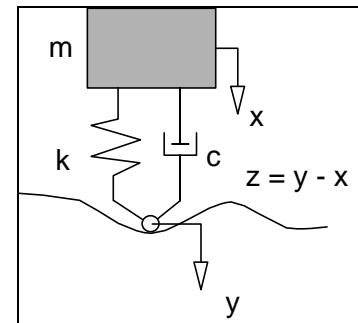


Fig. 12. Forced displacement

This equation has the same form as (2.3) and thus the same solution techniques are applicable.

In Fig. 13. an example is worked out in which the vibration transfer from a periodic load to the base of the 1-mass spring system is calculated. This is the situation encountered in vibration reduction problems in populated areas. The lower the natural frequency of the 1-mass spring system the better the excitation frequency components are reduced, or, in other words, are filtered out.

3.3 Wheel/rail forces

The wheel rail forces which act as dynamic loads to the track follow from the interaction between vehicle and track. If high frequency phenomena in relation to loads due to imperfections in wheel and rail geometry are the objective of the analysis the so-called P1 and P2 forces have to be considered as displayed in Fig. 14. The forces are described by the following equations (3):

$$P_1 = Q_{st} + 2a v \sqrt{\frac{k_H m_e}{1 + m_e/m_u}} \quad (2.15)$$

$$P_2 = Q_{st} + 2a v \sqrt{\frac{m_u}{m_u + m_t}} \left[1 - \frac{c_t p}{4k_t \sqrt{m_u + m_t}} \right] \sqrt{k_t m_u} \quad (2.16)$$

in which:

- 2α = total dip angle,
- m_u = vehicle unsprung mass,
- m_t = rail mass per unit length,
- m_e = effective track mass,
- k_h = Hertzian spring stiffness,
- k_t = track stiffness,
- c_t = track damping,
- v = vehicle speed in m/s.

The excitations originated from track induced forces are summarized in Fig. 15. For short waves in the order of centimeters rail corrugation, wheel irregularities and weld imperfections are the most important factors. For such high frequencies (up to 2000 Hz) the Hertzian contact spring between wheel and rail should be taken into consideration.

Rail rolling defects have wavelengths in the order of 3 m. The natural frequency of bogies are in the order of 20 - 25 Hz, whereas the sprung mass has a lowest natural frequency between 5 and 0.7 Hz and therefore primarily influences ballast and formation.

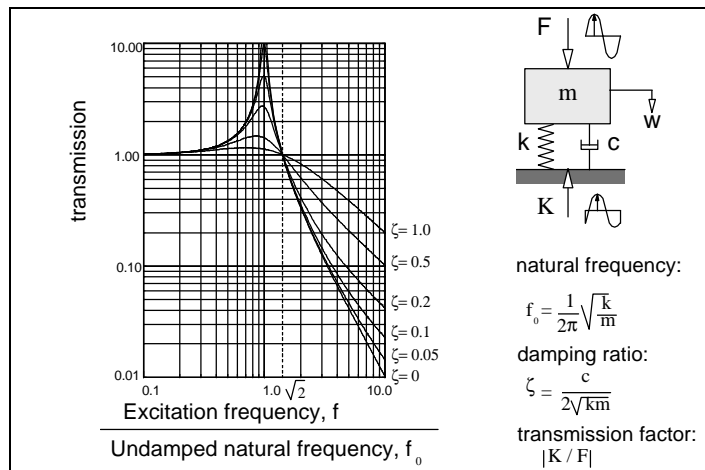


Fig. 13. Principle of vibration reduction

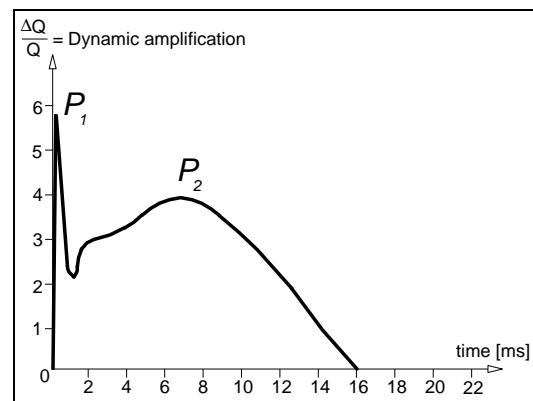


Fig. 14. Wheel/rail impact loads

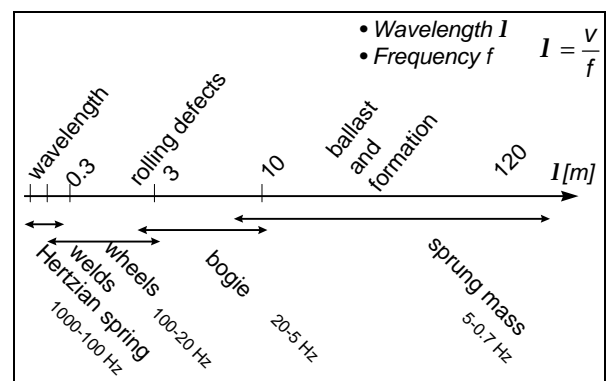


Fig. 15. Track loads in relation to frequency

3.4 Track modelling.

3.4.1 General considerations.

The type of interaction phenomenon to be described determines to a large extent the structure of the model and the degree of refinement. In the case under consideration here the track is of prime importance, however with the quality of the track being assessed on the basis of vehicle reactions.

To describe high frequency vertical vibrations associated with corrugations and poor quality welds use is made of a track model and a wheelset connected in the wheel/rail contact area via a Hertzian spring.

Vehicle reactions associated with low frequency track geometry are analyzed on the basis of a number of very simple models in which track stiffness is not taken into consideration. Running characteristics and aspects relating to stability are totally disregarded in such analyses.

3.4.2 Transfer function between track load and track displacement.

The track construction can be seen as a system consisting of rails, elastically supported via rail pads by sleepers spaced at a fixed distance. The sleepers are supported by a damped elastic foundation consisting of ballast plus formation.

Three models according to Fig. 16., which can be used to describe the track structure, are discussed below. The parameter values used in these models are shown in Fig. 17.

| | | |
|------------------------|-------------------|------------------------------------|
| $EI = 4.5 \cdot 10^6$ | $N \cdot m^2$ | rail bending stiffness |
| $M_w = 350$ | kg/m | unsprung wheel mass |
| $K_H = 1.4 \cdot 10^9$ | N/m | Hertzian contact spring stiffness |
| $m = 119$ | kg/m | track mass (single beam) |
| $m_1 = 54.43$ | kg/m | rail mass (double beam) |
| $m_2 = 157$ | kg/m | sleeper mass (double beam) |
| $k = 4 \cdot 10^7$ | $N \cdot m^{-2}$ | track stiffness (single beam) |
| $k_1 = 2.5 \cdot 10^8$ | $N \cdot m^{-2}$ | pad stiffness (double beam) |
| $k_2 = 4 \cdot 10^7$ | $N \cdot m^{-2}$ | foundation stiffness (double beam) |
| $c = 1.2 \cdot 10^5$ | $Ns \cdot m^{-2}$ | track damping (single beam) |
| $c_1 = 9 \cdot 10^4$ | $Ns \cdot m^{-2}$ | pad damping (double beam) |
| $c_2 = 1.2 \cdot 10^5$ | $Ns \cdot m^{-2}$ | foundation damping (double beam) |

Fig. 16. Survey of different parameter values used in the models

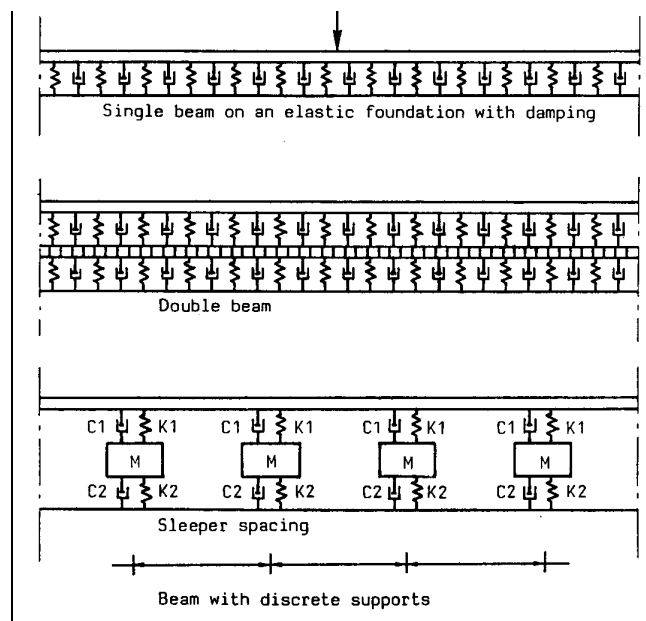


Fig. 17 Different models for describing dynamic track properties

3.4.3 Beam on an elastic foundation

The simplest model consists of a beam on an elastic foundation with a continuously distributed stiffness and damping, as shown in the drawing in Fig. 3.3 (a). The beam is modeled as a Euler beam, thus the rotational inertia and shear force deformation are disregarded. For a concentrated load at $x = 0$ with a magnitude of:

$$F(t) = Qe^{i2\pi ft} \quad (2.17)$$

the following differential equation applies:

$$Ely^{iv}(x,t) + m\ddot{y}(x,t) + c\dot{y}(x,t) + ky(x,t) = 0 \quad (2.18)$$

where primes denote spatial derivatives and dots time derivatives. The boundary conditions are:

$$Ely'''(0,t) = 0.5Qe^{i2\pi ft} \quad (2.19)$$

$$y'(0,t) = 0 \quad (2.20)$$

$$y(\infty,t) = 0 \quad (2.21)$$

The solution of this differential equation has the form:

$$y(x,t) = w(x)e^{i2\pi ft} \quad (2.22)$$

Thus (2.18) can be rewritten:

$$EIw^{iv}(x) + [k - 4p^2 f^2 m + i2\pi fc]w(x) = 0 \quad (2.23)$$

This differential equation is very similar to the one for the statically loaded and elastically supported beam presented in Fig. 18. The foundation coefficient k must, however, be replaced by the complex coefficient k^* according to:

$$k^* = \sqrt{[k - 4p^2 f^2 m]^2 + 4p^2 f^2 c^2} e^{i \arctan \frac{2\pi fc}{k - 4p^2 f^2 m}} \quad (2.24)$$

The displacement $w(x)$ is now also a complex quantity. For further considerations it is important to know the transfer function $H_r(f)$ between load and displacement at $x = 0$ according to:

$$H_r(f) = \frac{w(0)}{Q} \quad (2.25)$$

With $\beta = 1/L$, in which L is the characteristic length, the displacement at $x = 0$ is:

$$w(0) = \frac{Q}{8EI\beta^3} \quad (2.26)$$

Thus (2.25) becomes:

$$H_r(f) = \frac{1}{8EI\beta^3} \quad (2.27)$$

The value of β can be obtained from:

$$b^4 = \frac{k^*}{4EI} \quad (2.28)$$

Using the substitutions:

$$f_n = \frac{1}{2p} \sqrt{\frac{k}{m}} \quad (2.29)$$

$$x = \frac{c}{2\sqrt{km}} \quad (2.30)$$

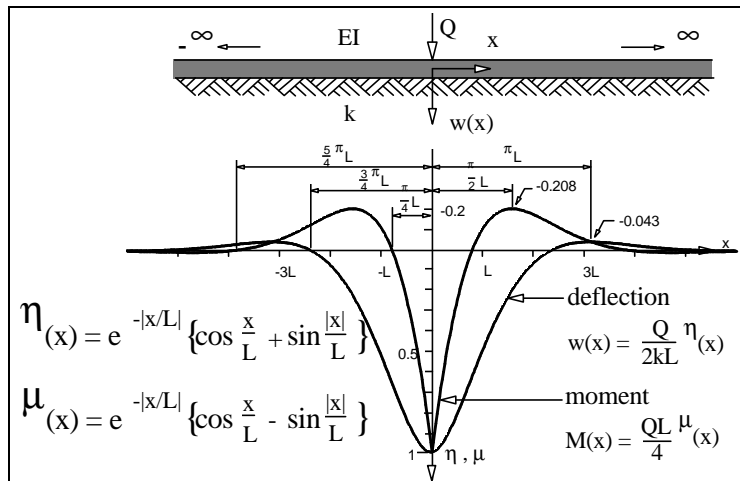


Fig. 18. Beam on an elastic foundation

and the formulae (2.24) and (2.28) the transfer function according to (2.27) can now be written as:

$$H_r(f) = \frac{1}{2kL} \left\{ \left[1 - \frac{f^2}{f_n^2} \right]^2 + 4V^2 \frac{f^2}{f_n^2} \right\}^{-\frac{3}{8}} e^{if} \quad (2.31)$$

$$f = -\frac{3}{4} \operatorname{atan} \left[\frac{2V \frac{f}{f_n}}{1 - \frac{f^2}{f_n^2}} \right] \quad (2.32)$$

In this equation L is the characteristic length. If f is zero the same static value is obtained, as with as with the static solution presented in Fig. 18., according to:

$$H_r(0) = \frac{1}{2kL} = \frac{L^3}{8EI} \quad (2.33)$$

The modulus of the transfer function is given by the term preceding the exponential function in formula (2.31), whereas (2.32) describes the argument. Both functions are represented in Fig. 19.

The correlation between this solution and that of the 1-mass spring system is striking. Both transfer functions have the same form only the order of the distributed system is 1.5 instead of 2. This shows up as the power $-3/8$, which is $-1/2$ for the 1-mass spring system. The phase approaches $-3/4 \pi$, instead of π , for high frequencies.

The complex characteristic length λ is obtained from (2.28), in which:

$$I = \frac{1}{b} \quad (2.20)$$

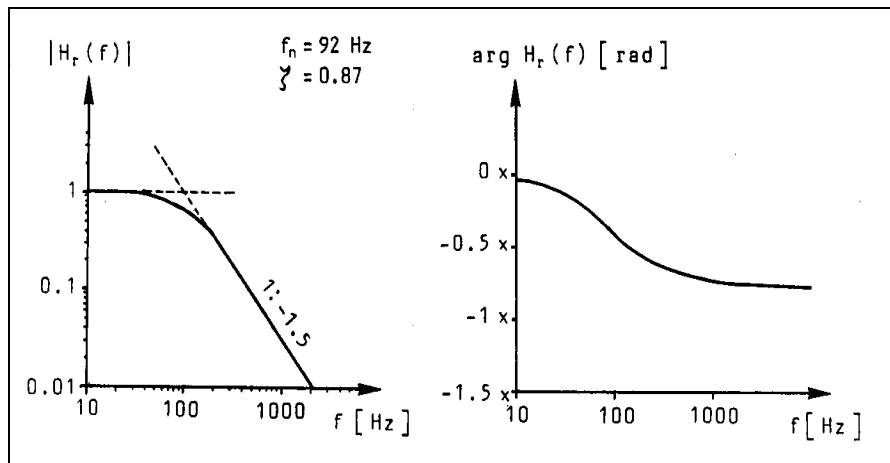
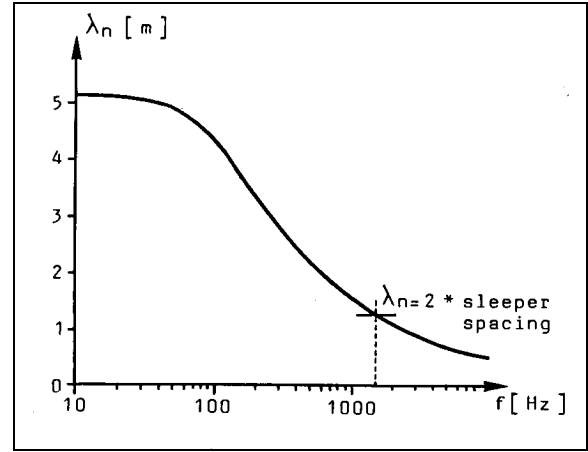


Fig. 19 Transfer functions for track modeled as a single beam

For small values of $f \lambda$ approaches L . To find the actual wavelength λ must now be multiplied by 2π . The modulus of this natural wavelength λ_n is therefore:

$$I_n = \left| \frac{2p}{b} \right| \quad (2.34)$$

and is plotted in Fig. 20. At 1500 Hz λ_n reaches a value of twice the sleeper distance (= 1.2 m). For higher frequencies the schematization based on a continuous support is thus no longer permissible.



3.4.4 Double beam.

When the track structure is schematized as a double beam Fig. 20. Natural wavelength versus frequency beam, as shown in Fig. 17 (b), in which the top beam represents the rail and the lower beam the sleeper, the displacement as a function of the load will also be determined. The upper beam, which represents the rail, has a distributed mass m_1 and a bending stiffness EI . The sleepers are represented as a continuous beam with a mass m_2 and a bending stiffness of zero. The connection between the two beams consists of the rail pads with a stiffness k_1 and a damping c_1 . The ballast contributes to the model with a stiffness k_2 and a damping c_2 .

The calculation is carried out by dividing the model into three parts, i.e. the rail, the rail pads and the sleepers. For each layer a separate differential equation is formulated. When combined, with the same boundary conditions as for the single beam model, the following transfer function is obtained:

$$H_r(f) = \frac{w(0)}{Q} = \frac{1}{8EIb^3} \quad (2.35)$$

in which:

$$b^4 = \frac{k_t^2 - 4p^2 f^2 m_1}{16EI} \quad (2.36)$$

where:

$$k_1 = \frac{A \cdot B}{A + B} \quad (2.37)$$

$$A = k_1 + i2pfc_1 \quad (2.38)$$

$$B = -4p^2 f^2 m_2 + k_2 + i2pfc_2 \quad (2.39)$$

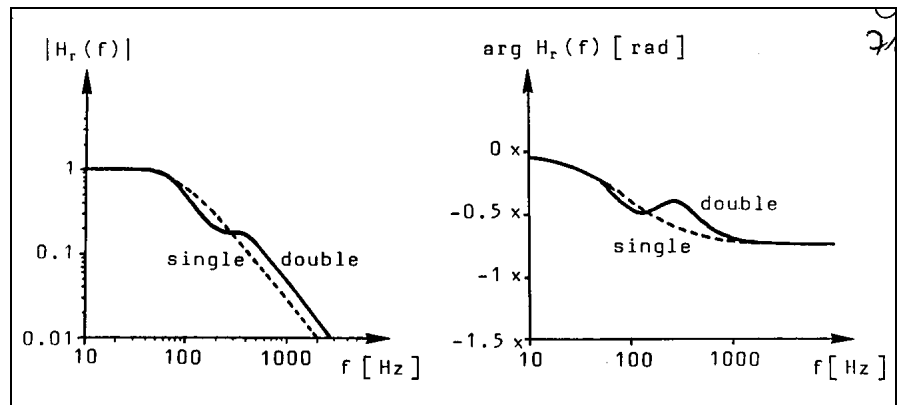


Fig. 21. Transfer function for track modeled as double beam

By numerical evaluation of these expressions the modulus and argument of H_r are found. Both functions are illustrated in Fig. 21. By way of comparison the functions for the single beam are also shown.

3.4.5 Discrete support.

The model in Fig. 17 (c), in which the rail is supported in a discrete manner, gives the best approximation. Such an approach also lends itself to the application of standard programs. These discrete and finite element method programs give great flexibility as regards load forms and support conditions.

3.5 Vertical wheel response.

3.5.1 Hertzian contact spring.

During vehicle/track interaction the forces are transmitted via the wheel/rail contact area. On account of the geometry of the contact area between the round wheel and the rail, the relationship between force and compression, represented by the Hertzian contact spring, is not linear. Since a description of the wheel/rail relationship using transfer functions requires that all components are linear the Hertzian spring must also be linearized. The relationship between force F and indentation y of the contact surface is:

$$F = C_H y^{3/2} \quad (2.40)$$

in which C_H is the Hertzian spring stiffness [$\text{Nm}^{-3/2}$]

The linearized value of the stiffness can be found by considering the relationship between the force and displacement increments around the static wheel load. The linearized Hertzian spring stiffness k_H is then:

$$k_H = \frac{dF}{dy} = \frac{3}{2} C_H^{2/3} F^{1/3} \quad (2.41)$$

Jenkins ea. [15] determined the C_H value for old and new wheels as a function of the wheel diameter. For a wheel diameter of 1 m and a static wheel load of 7.5 t a k_H value of $1.4 \cdot 10^9$ N/m is found for new wheels and $1.6 \cdot 10^9$ N/m for old wheels.

3.5.2 Transfer functions between wheel and rail.

Fig. 22. shows the model of a wheel which is connected to the rail via a Hertzian spring . From the equilibrium the following is obtained:

$$F_H + M_w \ddot{y}_w = 0 \quad (2.42)$$

With:

$$y_w = \hat{y}_w e^{12pft} \quad (2.43)$$

the transfer function of the wheel is obtained from (2.42) according to:

$$H_w(f) = \frac{\hat{y}_w}{F_H} = \frac{1}{M_w 4p^2 f^2} \quad (2.44)$$

In the following, the relationships between wheel displacement at axle box level and vertical rail geometry, as well as axle box acceleration and vertical rail geometry are examined. These relationships are important when analyzing phenomena associated with corrugations and poor quality welds. These transfer functions also formed the basis of the calculations which were carried out when designing the corrugation measuring system implemented in the track recording car of NS.

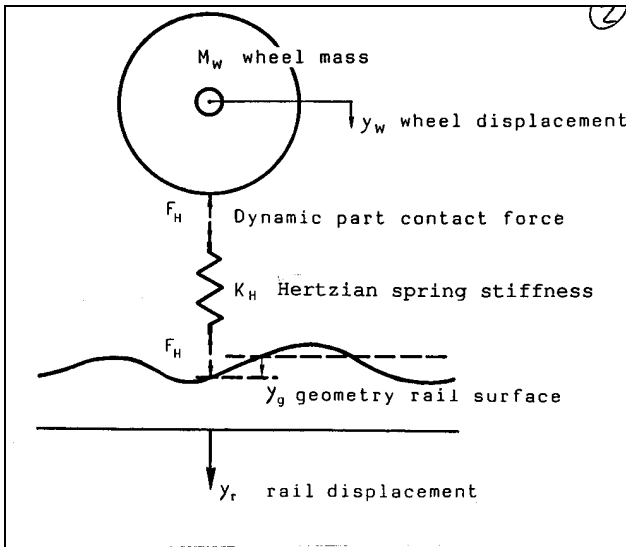


Fig. 22. Hertzian spring force acting between wheel and rail

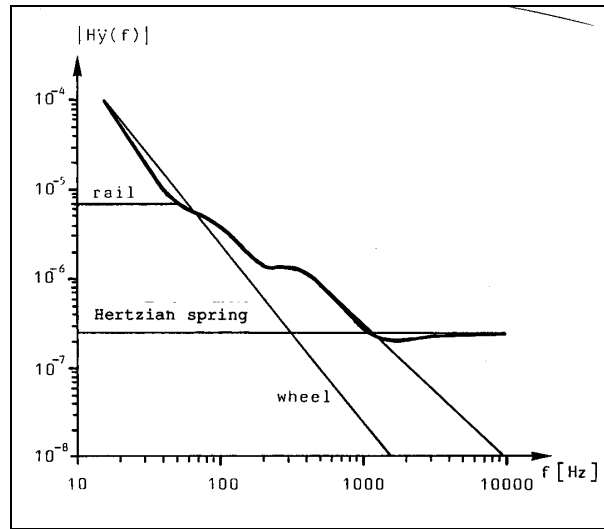


Fig. 23. 1 Transfer function between rail geometry and axle box acceleration

The relation between the interaction force F_H and the change in length of the Hertzian spring is determined by:

$$F_H = k_H [y_w - y_r - y_g] \quad (2.45)$$

in which:

y_w = vertical wheel displacement at the level of the axle box

y_r = vertical rail displacement under the effect of F_H

y_g = vertical rail geometry

k_H = linearized stiffness of Hertzian spring

F_H = dynamic component of wheel/rail force

If (2.6) is transformed to the frequency domain and the Fourier transforms are indicated in capital letters, the expression can be written as:

$$Y_g(f) = Y_w(f) - Y_r(f) - F_H(f) / k_H \quad (2.46)$$

Using the previously derived transfer functions for the wheel (2.44) and the rail (2.25), or (2.35), the wheel and rail displacements can be expressed in the wheel/rail force:

$$Y_w(f) = H_w(f) F_H(f) \quad (2.47)$$

$$Y_r(f) = H_r(f) F_H(f) \quad (2.48)$$

After substitution of both in (2.7) this expression becomes:

$$Y_g(f) = [H_w(f) - H_r(f) - 1 / k_H] F_H(f) \quad (2.49)$$

$$= H_1(f) F_H(f) \quad (2.11)$$

The relation between wheel displacement $Y_w(f)$ and rail geometry $Y_g(f)$ is now obtained by substitution of (2.8) in (2.11), which results in:

$$Y_g(f) = \frac{H_1(f)}{H_w(f)} Y_w(f) \quad (2.50)$$

By differentiating the wheel displacement twice according to:

$$\ddot{Y}_w(f) = -4p^2 f^2 Y_w(f) \quad (2.51)$$

and substituting this result together with (2.44) in (2.50) the relation between axle box acceleration and rail geometry becomes:

$$\begin{aligned} Y_g(f) &= M_w H_i(f) \ddot{Y}_w(f) \\ &= H_{\ddot{y}}(f) \ddot{Y}_w(f) \end{aligned} \quad (2.52)$$

in which:

$$H_{\ddot{y}}(f) = M_w \left[H_w(f) - H_r(f) - \frac{1}{k_H} \right] \quad (2.53)$$

This transfer function forms the basis of the measuring principle of the corrugation measuring system of NS and is illustrated in Fig. 23. in which the moduli of the various contributions are plotted, as is the modulus of the resulting transfer function. The contribution of the rail is calculated using the double beam model.

Fig. 23. shows that the wheel produces by far the greatest contribution in the frequency band up to about 50 Hz. The rail is mainly responsible for the behaviour in the 50 to 1000 Hz band and the Hertzian spring determines the behaviour above 1000 Hz.

Since corrugations appear predominantly between 10 and 1500 Hz it is clear that the track construction in particular has a very great influence. The question is whether, when measuring corrugations via axle box accelerations, the variation in track condition can be disregarded. This is examined by varying the track stiffness k_1 . Fig. 24. shows the various contributions made to the transfer function according to formula (4.15) for standard track with a stiffness k_1 , for track with a low stiffness of $0.5 k_1$ and for track with a high stiffness of $2 k_1$. Differences due to the characteristics of the track only show up in the frequency band between 60 and 200 Hz. As a result of system damping due to half-space radiation.

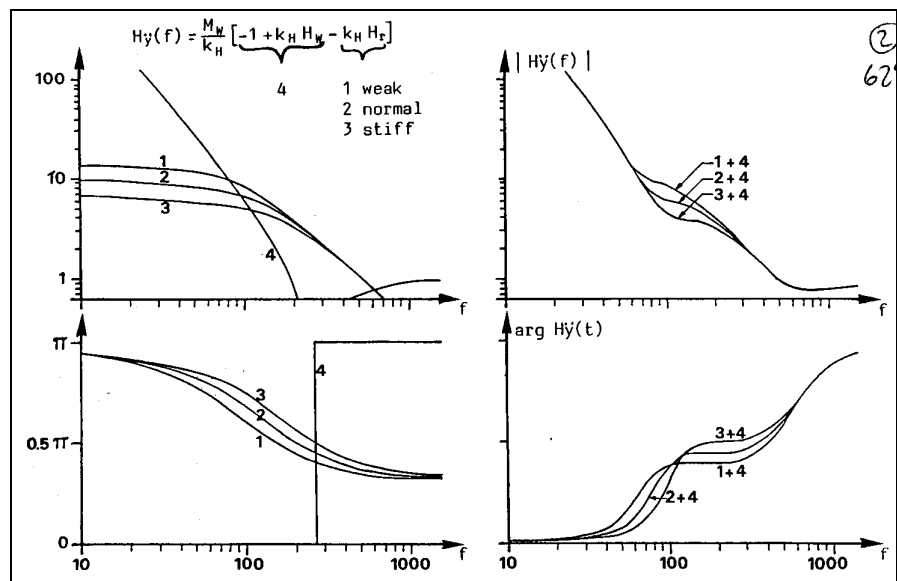


Fig. 24 Influence of track stiffness on the transfer function

3.5.3 Analysis of paved-in tram track structure

| | | |
|----------------------------|-----------|--------------------------|
| Rail (Nikex profile) | mass | 52.75 kg/m |
| | I | $261.637e-8 \text{ m}^4$ |
| | A | $6720e-6 \text{ m}^2$ |
| Rubber supports | stiffness | 100e6 N/m/m |
| | damping | 30e3 s/m/m |
| Concrete slab | height | 0.18m |
| | E | $3e10 \text{ N/m}^2$ |
| | ν | 0.45 |
| | ρ | 2400 N/m^3 |
| Asphalt | height | 0.12 m |
| | E | $4e9 \text{ N/m}^2$ |
| | ν | 0.45 |
| | ρ | 2300 N/m^3 |
| Foundation (3 sand layers) | height | 0.12 m each |
| | E | $2e8 \text{ N/m}^2$ |
| | ν | 0.45 |
| | ρ | 1820 N/m^3 |

Fig. 25. Properties of Nikex construction

Instead of working with analytical models it is often more convenient to use finite element models or discrete element models due to the flexibility in boundary shapes. The studies related to the earlier described project on light rail track dynamics were carried out using the TILLY discrete element program developed at TU Delft.

A dynamic analysis may consist of various levels of sophistication, varying from a quasi-static approach to the determination of total stresses under moving vehicles or complete trains. As a first step the TILLY analyses were used to determine the dynamic characteristics of the track, i.e. analyzing the susceptibility of the track to specific frequencies of the load spectrum generated by passing trains. Coincidence of excitation frequencies, either consisting of natural frequencies of rolling stock components, or frequencies induced by geometrical imperfections of wheel and rail, should be avoided.

In the study referred to in [1] a stratified track model was developed according to Fig. 26.

The model can be described as follows. In the

longitudinal direction of the track a concrete slab of 30 cm thickness is situated as foundation. On top of this slab grooved rails Ri60 are positioned supported at intervals of L m.

Between rail and slab elastic pads, characterized by a discrete spring and damper per support, are mounted. The concrete slab is supported by an asphalt layer on top of 3 elastic layers describing the soil properties. The layer properties used for modeling a Nikex construction, comprised of prefabricated concrete slabs, supported by an asphalt layer and a number of soil layers, are presented in Fig. 25..

The dynamic analysis of this Nikex construction consisted of determining the response due to a pulse shaped load. The time function of load and displacement, depicted in Fig. 27., were Fourier transformed with the help of MATLAB to produce the transfer function as a function of frequency, which is displayed in Fig. 28.. The frequency response peak at about 200 Hz is due to the natural rail vibration on the rubber support.

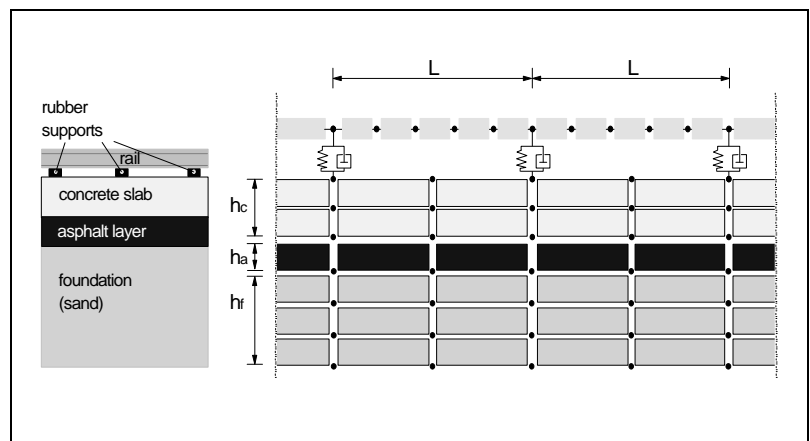


Fig. 26. Track model to describe Nikex construction

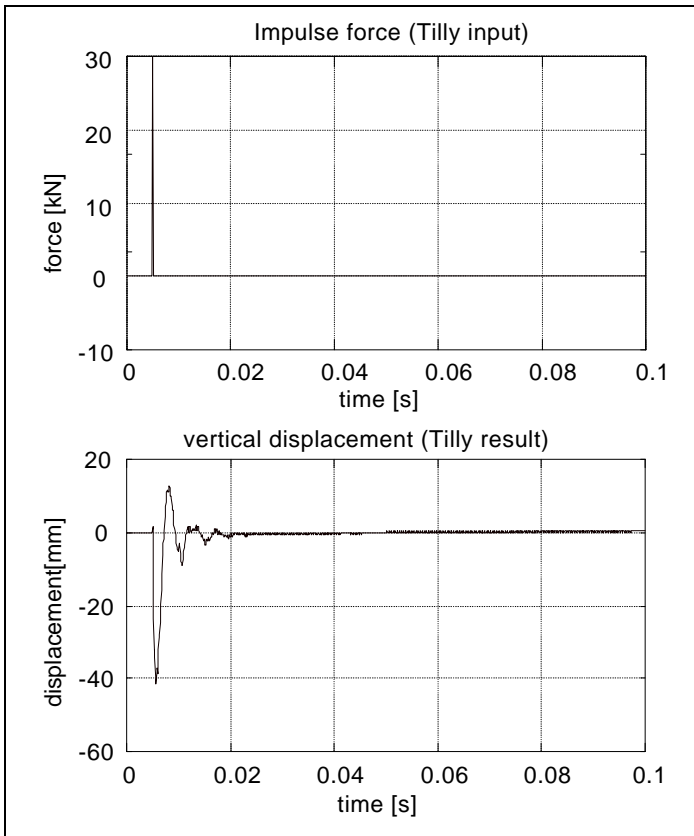


Fig. 27. Displacement response of Nikex construction, due to an impulse load, determined with TILLY

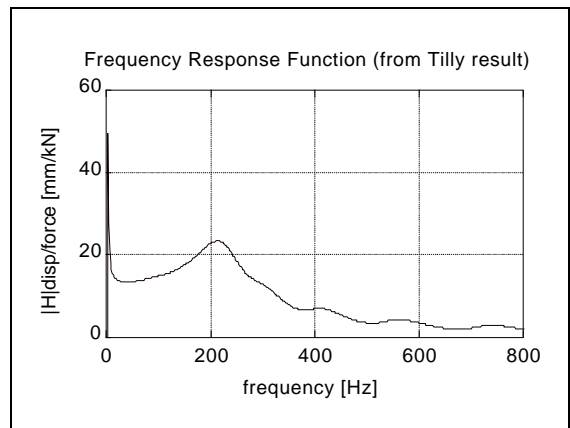


Fig. 28 Transfer function of Nikex construction determined with FFT from Tilly

Apart from the TILLY program TU Delft uses a number of other models for dynamic analysis, i.e.:

- RAIL: a moving load program comprised of a Timoshenko beam on a Winkler/Pasternak foundation [17];
- SPOOR: a multi layer model, which calculates steady state response to moving loads [18];
- DIANA [16] and GT-STRUDL: 3-dimensional finite element programs.

3.6 Embedded rail construction

The embedded rail construction (ERC) is generally considered as a very serious alternative to ballasted track for the new high speed track, southern branch, in the Netherlands.

To assess the dynamic properties of ERC a first test series was conducted recently on a 50 cm rail length embedded in corkelast. A heavy excitation hammer was used to induce a free vibration of the rail. Two accelerometers were attached to the rail in the vicinity of the loading point to record the response.

Fig. 29. shows the time recordings force and vibration which resemble very much the rail pad test recordings in Fig. 20.

In Fig. 30. first the auto spectra are given of the input and output signal respectively. The force auto spectrum shows the frequency content which depends on the hardness of the hammer tip. If a harder hammer tip would be used, the frequency content would increase and higher frequencies in the system would be activated.

The frequency response function (here the inertance function) is also shown in Fig. 30. with its coherence function based on five measurements. The value of the coherence function around the inertance peak value about 180 Hz is excellent.

Fig. 31. shows the result of the curve fitting procedure for the two accelerations based on a single degree-of-freedom

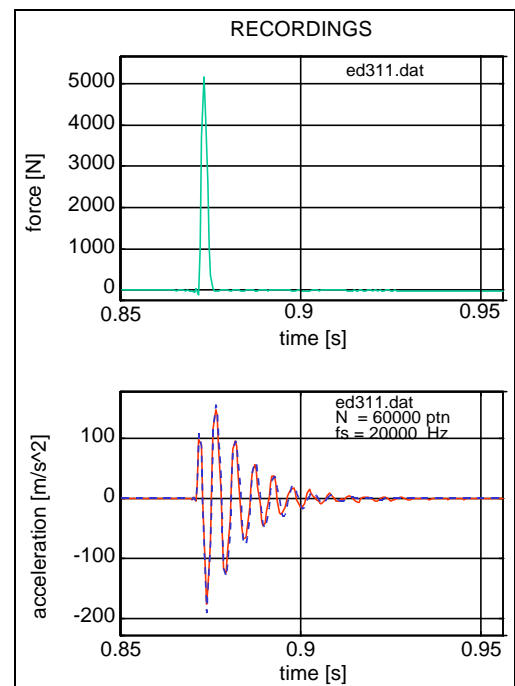


Fig. 29. Time recordings embedded rail test

system model. The results are almost identical as was to be expected.

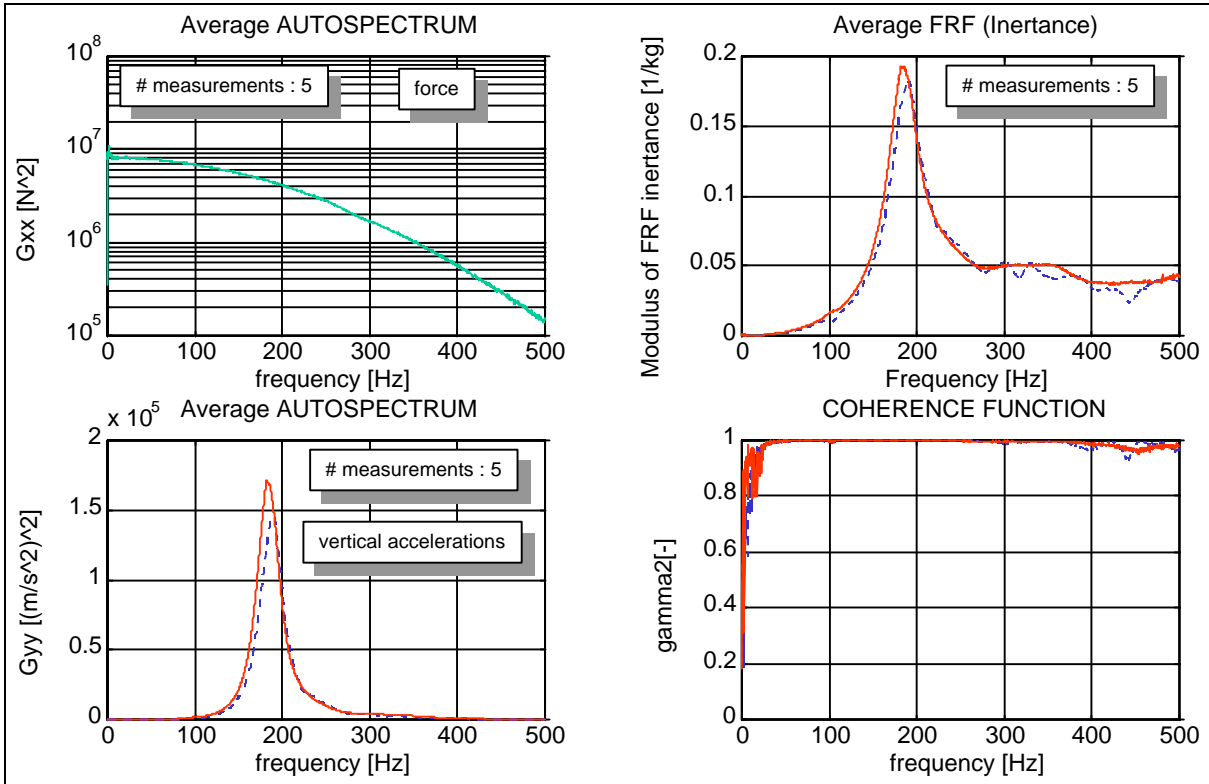


Fig. 30. Auto spectra and inertance function embedded rail test

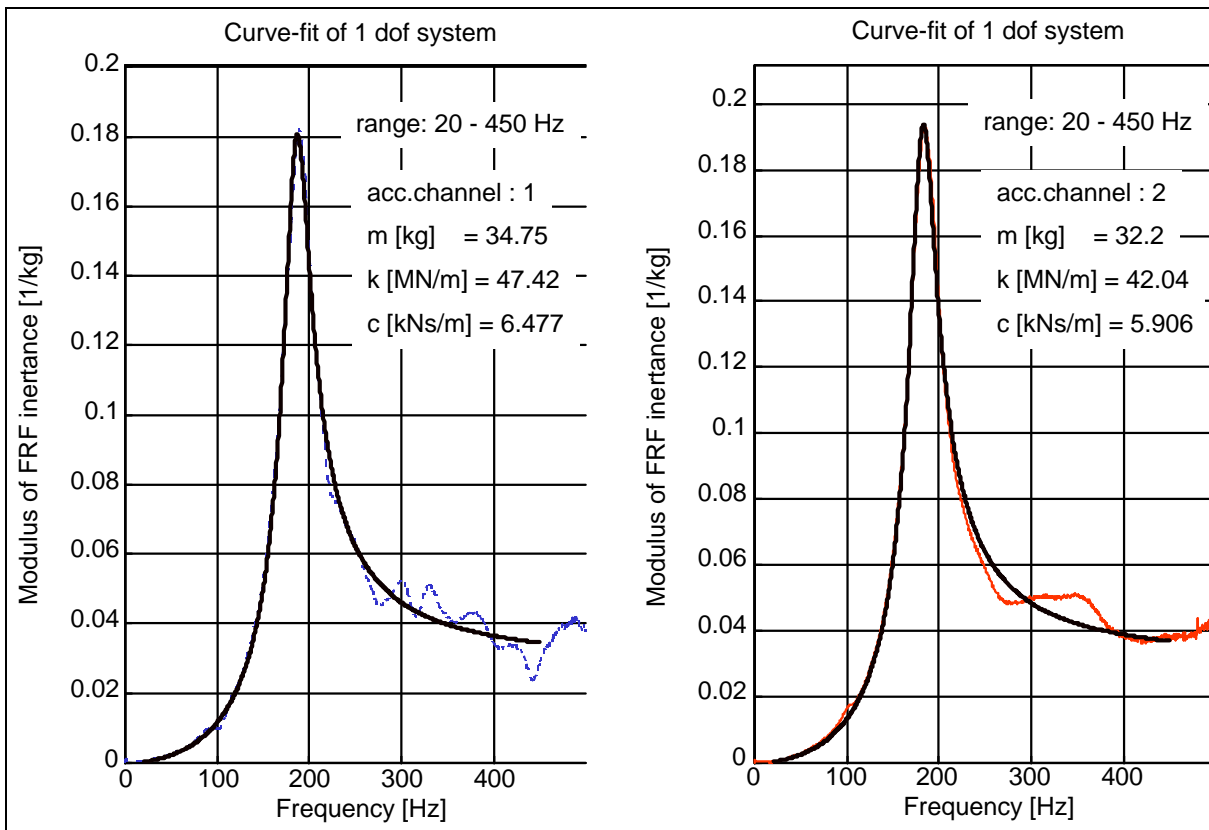


Fig. 31. Curve fit results embedded rail based on single degree-of-freedom system model

4. REFERENCES

- [1] Scheepmaker, P.N.: 'Concrete in Railway Structures', Report 97-3a, C.R.O.W., March 1997.
- [2] Esveld, C.: 'Innovation for the control of infrastructure maintenance', Rail International/Schienen der Welt, February 1997.
- [3] Esveld, C.: 'Lecture notes Railway Engineering (in Dutch)', TU Delft, 1996
- [4] Esveld, C. and Kok, A. W. M.: 'Dynamic Behaviour of Railway Track', Railway Engineering Course TU Delft, Department of Civil Engineering, November 1996.
- [5] Esveld, C.: 'Modern Railway Track', MRT-Productions, ISBN 90-800324-1-7, 1989.
- [6] Darr, E. and Fiebig, W.: 'Stand der Entwicklung und des Einbaus der Festen Fahrbahn', ZEV+DET Glas. An. 120 (1996) Nr 4. April pp 137-149.
- [7] Henn, W.D.: 'System comparison: ballasted track - slab track', Rail Engineering International 1993 2 pp 6-9.
- [8] Leykauf, G. and Mattner, L.: 'Ballastless track structures in Germany', European Railway Review September 1995 pp 73-78.
- [9] Hilliges, D., 'Feste Fahrbahn-Konstruktionen. Perspektiven für Strecken mit hohen Geschwindigkeiten oder hohen Achslasten.', Der Oberbau Maart 1988 pp 25-29.
- [10] Fastenau, W., Widmann, H. and Jetter, A.: 'Die Feste Fahrbahn Bauart Züblin', EDTR 40(1991) H.7 Juli pp 443-449.
- [11] Eriean, J.: 'La Voie. Essais de voie sans ballast en France et à l'étranger', pp 63-72.
- [12] Hofmann, Ch.: 'Ballastless track applications in tunnels, experience on SFR', SBB/CFF/FFS Permanent way department, 13-06-95.
- [13] Ando, K., Miura, S. and Watanabe, K.: 'Twenty Years' Experience on Slab Track', QR of RTRI Vol. 35 No. 1 Feb. 94.
- [14] Esveld, C., e.a.: 'Estimation of Dynamic Track Properties', Rail Engineering International, Edition 1996/2
- [15] Jenkins et al.: 'The effect of track and vehicle parameters on wheel/rail vertical dynamic forces', REJ, January 1974.
- [16] Suiker, A. S. J.: 'Dynamic behaviour of homogeneous and stratified media under pulses and moving loads', TU Delft, Report 7-96-119-1, July 1996.
- [17] Kok, A.W.M.: 'Moving loads and vehicles on a rail track', TU Delft report 03.21.1.22.23, May 1996
- [18] Kok, A.W.M.: 'Moving loads', TU Delft report 03.21.1.22.05, December 1995